Magnetic field and beam position measurements for the ECR ion source Alice

V.Batalin*, M.Cavenago, T.Kulevoy*, V.Stolbunov* and A. Vassiliev*
Lab. Naz. di Legnaro INFN, via Romea n 4, I-35020 Legnaro (PD) Italy
*ITEP, Bolshaja Cheremushkinskaja n 25, 117259 Moscow, Russia

Abstract

During a long shutdown of Alice ECR ion source it was possible to measure several misalignments influencing the beam quality, and to design the proper diagnostic for future operation. The hexapole fields B_r and B_ϑ were mapped in r, z, ϑ by a high precision probe, while B_z was construed by a Bessel-Fourier formula. After measuring the extractor misalignment with a theodolite, the electrostatic field was obtained with a 3D numerical simulation. A versatile compact beam scanner is designed, giving formulas to retrieve beam moments and therefore emittance.

1 INTRODUCTION

The alignment of the magnetic axis of an ion source and of the electrostatic axis of its extractor is the major requirement for a good quality of the ion beam. This paper records the measurements of hexapole magnetic field and of mechanical misalignment that we take during a long shutdown of the source, and discuss their relevance to beam steering. We present the design concept of a compact beam scanner (CBS), primarily intended to verify whether a new extractor will stay well aligned while it is displaced. Since slits are not practical, we propose some formulas to retrieve as much information about emittance as possible from current measurement alone.

We will use both a cylindrical coordinate system r, ϑ, ℓ and a cartesian system x, y, ℓ , where ℓ (or Z) lays along the source geometric axis (fig. 1); z will be the complex variable $z = x + iy$. In a region free of current and magnetic material, say a cylinder of radius a and length L, the magnetic field can be obtained as $\mathbf{B} = -\mathrm{grad}\,\phi$, where the magnetic potential can be expanded in a Fourier-Bessel series [1]:

$$\phi = 2\sum_{n=1}^{\infty} \sin k_z \ell \sum_{m=-\infty}^{\infty} \exp(im\vartheta)\, \frac{I_m(k_z r)}{k_z^m}\, c_m(k_z) \qquad (1)$$

Here $k_z = n\pi/L$ and the case of antisymmetric conditions imposed at $\ell = 0$ and $\ell = L$ was considered. The hexapole of an ECR is purposely designed to give a strong $c_3(k_z)$ components, while other c_m terms comes from: 1) errors in construction of the hexapole; 2) different magnetization of hexapole bars. In particular, a misalignment of ECR plasma chamber and the whole hexapole will give c_0 , c_1 and c_2 terms.

2 HEXAPOLE MEASUREMENTS

To measure field, we use a transverse field probe based on Hall effect, whose sensing area is 1.6 mm (in ℓ) by 4 mm by 0.1 mm, and axis uncertainty better than 1^0. We aimed to control the probe center transverse coordinates r, ϑ within 0.2 mm and the axial one within 0.5 mm, with tilting of probe limited to 1^0. To that purpose we enclosed the probe into 20 by 10 mm rectangular section stainless steel tube, which is supported by two slits, placed at the ends of Alice central section. Each slit is carved into a plexiglas disk, bolted by 12 screws to Al adapter, secured to a CF flange. Since one end has a CF100 flange, while the other end features a CF200 one, the two adapters can rotate in 45 degree steps only. Combining this rotation with the disk steps we obtain 15 degrees steps, corresponding to the 24 bars that constitute our hexapole. Alignment of flanges was checked with a theodolite.

Actually we cut 4 slits in each disk, allowing us to measure: B perpendicular to the probe at $r = 0$ (data set 1); B_ϑ respectively at $r = 0.6$ cm, 1.8 cm and 2.4 cm, (data sets 2,3 and 5); B_r respectively at 1.8 cm and 2.4 cm (data sets 4 and 6).

By sliding the probe into the slit, after verifying each time the probe zero, field values at different z can be easily measured with resolution of 0.05 G, 0.10 G or 0.20 G , depending on the range used. Note that field at axis is low, so that 0.05 G resolution is possible on the whole data set 1. Each data set contain values taken at N_ϑ azimuthal position (12 or 24) and at N_z axial steps ($\ell = \ell_0, \ldots, \ell_{N_z-1}$) on the axis (step length was $s_z = 1$ cm and $N_z = 35$).

2.1 Data processing and results

The region of our measurements can be enclosed in a cylinder as required by eq. 1; the antisymmetric condition corresponds to assuming negative images of the hexapole. The relation between this imaginary cylinder, and the region of measurement can be adjusted for optimum rendering of the field tails; anyway the simpler choice $\ell_0 = s_z = 1$

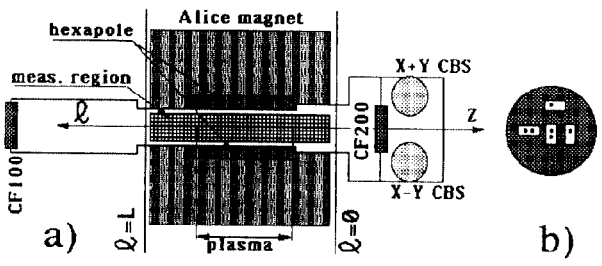

Figure 1: a) Overview of Alice source and region of magnetic measurements; b) plexiglas disk (detail)

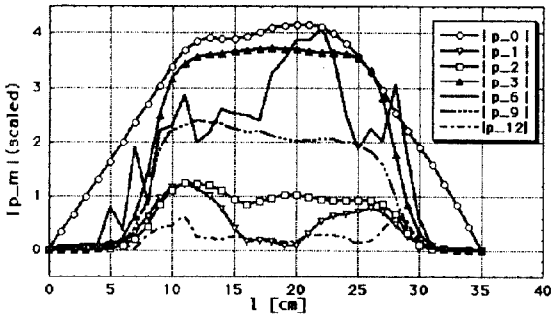

Figure 2: The (rescaled) multipole coefficient p_m for $r = 2.4$ cm and $m = 0, 1, 2, 3, 6, 9, 12$; maxima are respectively 414 G cm, 124 G cm, 124 G cm, 3720 G cm, 4 G cm, 24 G cm, 0.67 G cm

cm and $L = \ell_{N_z-1} + \ell_0 = 35$ cm is satisfactory. This is due to the fact that ECR cavity extends from $\ell = 8$ cm (extractor side) to $\ell = 26$ cm (microwave injection side), where image effects are negligible.

The coefficient $c_m(k_z)$ can be determined from measured data by inverting eq. (1), provided that, in the sum of eq. 1, we bound $n \leq L/s_z = 35$ and m in the closed interval $[1 - N_\vartheta/2, N_\vartheta/2]$ in order to avoid aliasing. Besides this general limitation, the data set taken at $r = 0$ can be used to determine the $m = 1$ (and $m = -1$) coefficient only, with the advantage of giving a more precise value. Every coefficient $c_m(n\pi/L)$ is determined separately from each data set, and final result is obtained by averaging values from all sets.

From the average value of the c_m coefficient and eq. 1 we can obtain every field value, in particular the combinations

$$p_m(r,z) = 2f_m \sum_{n=1}^{L/s_z} \sin(k_z\ell)\frac{I_m(k_z r)}{k_z^m} c_m(k_z) \qquad (2)$$

(with $f_m = 2$ but for $f_0 = f_{N_\vartheta/2} = 1$), which are plotted in fig 2 and enter in the expressions of ϕ and B_ϑ ; for example:

$$B_\vartheta = \Re \sum_{m=0}^{N_\vartheta/2} i\,m \exp(im\vartheta)\, p_m(r,z)/r \qquad (3)$$

Apart from expected dipole and quadrupole coefficients, we note a $m = 0$ coefficient (the monopole), which may well be a residual of solenoid magnetization or a probe size effect and must be confirmed by later analysis.

Note that even at $r = 2.4$ cm the $m > 3$ components are very small, as they should according to the Halbach construction used in hexapole design; this also verifies that no hexapole bar has a largely defective magnetization.

A definition of magnetic axis adequate to imperfect hexapoles is missing in literature to our knowledge. While a complete and formal definition cannot be given here for lack of space, still we can prove the basic result that we have two privileged lines that can be considered as axes and propose an intuitive definition of axis.

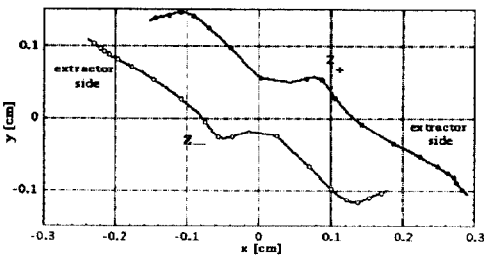

Figure 3: View of nodal lines $z_\pm(\ell)$ from the extractor side; a point is marked for each 1 cm.

We first consider the point(s) where $B_x = B_y = 0$ at given ℓ, which we call nodal points. Near the geometrical axis, these field can be computed by taking leading terms in I_m/k_z^m expansion of eq. (1); we obtain $\mathbf{B} = -\text{grad}\,\Re[V]$ with:

$$V = \Phi_0 + \Phi_1 z + \tfrac{1}{4}\Phi_2 z^2 + \tfrac{1}{24}\Phi_3 z^3 + \ldots \qquad (4)$$

where $z^m = (x+iy)^m$ comes from $\exp(im\vartheta)r^m$ and

$$\Phi_m(\ell) = 2\sum_{n=1}^{L/s_z} \sin(k_z) c_m(k_z) \qquad (5)$$

Since the simplified expression of V of eq. 4 is a function of a complex variable, the nodal equation becomes simply:

$$0 = \frac{\partial V}{\partial z} = \Phi_1 + \tfrac{1}{4}\Phi_2 z + \tfrac{1}{8}\Phi_3 z^2 \qquad (6)$$

which has evidently two solutions at each ℓ, called $z_+(\ell)$ and $z_-(\ell)$ as usual.

We find out that the source has two nodal lines. Therefore we prefer to think that the central structure of an imperfect ECR is not an axis, but a band limited by those nodal lines. If only one line is desired as the reference axis, that line should be defined as the fluxline which lays in the band and passes near $z = (z_+ + z_-)/2$ at $\ell = L/2$.

In fig. 3 the front view of the nodal lines is shown. Since nodal lines fall inside the extraction hole, no dramatic modification of beam current and quality can be forecast on the basis of field misalignment.

3 BEAM TRAJECTORY

We easily verified that the puller electrode was misaligned respect to the extractor hole by $e_y = 1.7$ mm in a $L_1 = 3.4$ cm distance. Let Z be the desired beam axis ($-\ell$ of previous section). We can compute the external electrostatic potential $\phi^{\text{ext}}(x, y, Z)$ due to this misalignment with the code TOSCA (by Vector Fields, Oxford).

We consider the average coordinates of a beam $\bar{x}$ and $\bar{y}$ of the beam at a given ℓ , so that the repulsion among ions gives no net effect, leaving only the attraction towards walls due to image charges. Neglecting these image charges in first approximation, we can easily track the centroid orbit: we obtain a divergence $\mathrm{d}\bar{y}/\mathrm{d}Z = 0.022$ rad. This

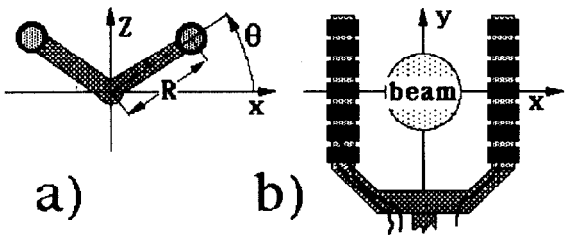

Figure 4: a) Top view of an x-CBS; b) front view

divergence is large (and is underestimated by neglecting image forces). We plan to reduce the misalignment to $e_y = 0.2$ mm .

4 NEAR SOURCE CBS

To reliably diagnose the behaviour of future extractors we need to measure $\bar{x}$, $\bar{y}$ near the ECR source. Suppose for example that we move the extractor to adjust focusing: if we observe a worst beam transport, we need to know whether the beam is defocused or just the extractor rotated while it was pulled or pushed into the new position.

We consider a class of CBSs similar to the well known rotating wire scanner (though rotated in discrete steps). Even so, several interesting question arose during design. The first requirement for this CBS is to fit the allocated space (12 cm by optic design). This makes the determination of the phase space distribution difficult. Secondly, the device must be easily extracted from ECR beam. Thirdly, we would like to attempt to monitor some characteristic of the source, as for example whether the beam is stable and therefore follows the same path, or is unstable, and then its path can fluctuate; simple beam pickups are well known to ECR community [2].

The two latter requirements lead us to imagine a one or two tine fork shaped detector (see Fig 4), whose tine spacing be greater than the expected beam size D_b.

Let Z_0 be the center of device, R the distance of one tine from rotation axis and θ the angle between the tine plane (the plane containing one selected tine and the fork axis) and the plane $Z = Z_0$. When $\theta \cong 90^0$ the beam pass safely through; when the angle is a little less than $\arccos(D_b/2R)$ the beam passes through marginally, so that path fluctuations are detected. When $|\cos\theta| < D_b/2R$ part of the beam current is collected, depending on position.

In the actual device we will fit a $x-y$ and $x+y$ CBS by a trick, but for the sake of simplicity here let us discuss a x-CBS, where the fork is vertical (i.e. y is axis of rotation). Also we will segment each tine into several isolated pills, separately connected to external electronics, to get some information on y coordinates; but let us assume that tines are infinitely long in the y direction; that is equivalent to consider only the xx' phase space distribution $f(x, x'; Z)$. We pose: $F(x, x') = f(x, x'; Z_0)v_Z$.

Each tine will have a radius $a \cong 4-5$ mm, that allows to collect more current, but be must accounted for in the theory. The current impinging per unit length (on one tine avoiding the shadow of the other) will be

$$I(\theta) = \int \mathrm{d}x' \int_{x_-}^{x_+} \mathrm{d}x F(x, x') \qquad (7)$$

where the integration limit depends on angle θ as

$$x_\pm = R\cos\theta + Rx'\sin\theta \pm a\sqrt{1+x'^2} \qquad (8)$$

The more natural data processing is integrate I with some weight $g(\theta)$ since this gives a linear functional of F :

$$I[g] \equiv \int I(\theta)g(\theta)\mathrm{d}\vartheta = \int \mathrm{d}x\mathrm{d}x' w_g(x, x')F(x, x') \qquad (9)$$

where the resulting phase space weighting function is

$$w_g(x, x') = G(\theta_+^1) - G(\theta_-^1) + G(\theta_+^2) - G(\theta_-^2) \qquad (10)$$

Here $\theta_+^{1,2}$ are the two functions of x, x' obtained by inverting x_+ from eq. (8) and G is the primitive function of g . By choosing appropriately g , $I[g]$ can approximate some particular functionals of F , as the total current $\int \mathrm{d}x\mathrm{d}x' F$, which corresponds to $w_g = 1$. In particular $g = |\sin\theta|$ gives $w_g = 4a/R\sqrt{1+x'^2}$ (for $|x| \leq R-a$), which is approximately a constant on the whole beam, unless we consider unrealistic beam divergences greater than 30^0. Similarly $g = \sin\theta$ gives $w_g \cong -4axx'/R^2(1+x'^2)$, showing that $I[|\sin\theta|]$ is roughly proportional the average of xx' :

$$\overline{xx'} = -R\, I[\sin\theta] \,/\, I[|\sin\theta|] \qquad (11)$$

By inspection of plots of w_g we also found:

$$\overline{x} \cong R\,\frac{I[\cos\theta]}{I[|\sin\theta|]} \qquad \overline{x'} \cong \frac{I[\sin 2\theta]}{2\, I[|\sin\theta|]} \qquad (12)$$

From eqs. 11 and 12 we can also compute the emittance $\epsilon = \overline{xx'} - \overline{x}\,\overline{x'}$. The averages implied by eq. 9 may be done analogically, or preferably by computer. Choosing different g may improve the approximation of eqs. 11,12.

Before starting the construction of the final device in Legnaro, several models are being studied in Moscow; light is used to simulate the drift of particle beams. In particular, it is investigated whether more information on phase space distribution can be obtained when one tine is in the shadow of the other, which was not treated in the above theory. An improved determination of average emittance is possible, especially when assumption on beam shape can be made [3]. Also we are developing a miniature profile meter (20 by 30 by 50 mm size), featuring slits for phase space measurement, to be used in alternative to the CBS.

In fig. 4 we show some design detail of CBS. Note that each tine is constituted by several annular electrodes, and wires are connected inside; the center is to be filled by some vacuum ceramic. Note also that an angle of 110^0 is made between the two tine planes, so that we may immerse in the beam only one tine (as required by eq. 9 where shadow effect must be avoided).

5 REFERENCES

[1] M.Cavenago, *Nucl. Instr. Meth.*,A311,19(1992)

[2] T.Antaya, private communications.

[3] I.M.Kapchinsky, "The particle dynamics in linacs", Atomizdat, Moscow, 1966